Thin Solid Films 517 (2009) 6396–6400

Contents lists available at ScienceDirect

Thin Solid Films

journal homepage: www.elsevier.com/locate/tsf

# Surface photovoltage investigation of recombination at the a-Si/c-Si heterojunction

L. Korte [a,*], A. Laades [a,b], K. Lauer [b,c], R. Stangl [a], D. Schaffarzik [a], M. Schmidt [a]

[a] Helmholtz-Zentrum Berlin für Materialien und Energie, Abteilung Silizium-Photovoltaik, Kekuléstr.5, D-12489 Berlin, Germany
[b] CiS Institut für Mikrosensorik GmbH, SolarZentrum Erfurt, Konrad-Zuse-Str. 14, D-99099 Erfurt, Germany
[c] TU Ilmenau, Institut für Physik, Weimarer Str. 32, 98693 Ilmenau, Germany

ARTICLE INFO

Available online 21 February 2009

*Keywords:*
Surface photovoltage
Band bending
Interface defects
Amorphous/crystalline heterojunction

ABSTRACT

We investigate the use of time-resolved surface photovoltage (SPV) transients as a means to determine band bending and recombination properties at amorphous/crystalline silicon (*a*-Si:H/*c*-Si) heterojunctions. Experimentally, it is shown that for *a*-Si:H film thicknesses above ~6 nm, SPV transients do not depend on the film thickness anymore. On this basis, a simple numerical model is proposed that consists of a single rechargeable gap state on the *c*-Si wafer surface, into which the properties of the *a*-Si:H/*c*-Si interface and the adjacent *a*-Si:H are lumped. It is shown that this model can reproduce all principal features of high excitation SPV transients, i.e. an initial fast decay shown to be due to Auger recombination, a plateau region for high injection conditions and a fast decay when the sample returns into low injection and the defect states are recharged. Under sufficiently high excitation, the SPV saturates at a value that is determined by the *a*-Si:H/*c*-Si interface band bending in the dark. From the slope of the transient decay, defect parameters (density, energetic position) can be extracted.

© 2009 Elsevier B.V. All rights reserved.

## 1. Introduction

Amorphous/crystalline silicon heterojunctions produced by plasma enhanced chemical vapour deposition (PECVD) of ultrathin (5–10 nm) hydrogenated amorphous silicon layers, *a*-Si:H, on crystalline silicon substrates, *c*-Si, are an interesting concept for high-efficiency solar cells on monocrystalline wafers, and to realize large area heterojunction cell concepts on for low-cost thin-film silicon. For those cell types, in order to achieve high efficiencies, it is necessary to suppress interface recombination at the *a*-Si:H/*c*-Si interface. We have shown previously [1], that this can be achieved by decreasing the density of interface defect states $D_{it}(E)$ of the *a*-Si:H/*c*-Si interface and/or by increasing the c-Si band bending $q\varphi_{s0}$. Low $D_{it}$ can be obtained by reducing the *c*-Si surface defect density prior to *a*-Si:H deposition, and by choosing optimized *a*-Si:H deposition conditions [2], while the band bending is adjusted by the *a*-Si:H doping. The *a*-Si:H doping level has to be chosen as a trade-off between high band bending and high density of *a*-Si:H gap states at increased doping levels, which lead to enhanced recombination in the *a*-Si:H [3]. All those optimizations profit greatly from a tool to characterize the *a*-Si:H/*c*-Si interface recombination. To this end, we have been using surface photovoltage measurements (SPV), especially in the time-dependent and intensity-dependent modes (TD-SPV/ID-SPV) [4,5] and references therein], as a "fingerprinting" method to monitor the electronic properties of the *a*-Si:H/*c*-Si effective interface. With the present paper, using numerical simulations, we aim at a refined understanding of the mechanisms that determine the transient decrease of photovoltage over time after the short illumination light pulse. This will allow to extract *a*-Si:H/*c*-Si interface recombination properties that can be compared, for adequate sample structures, to those obtained by other means such as quasi-steady state and microwave photoconductance decay (QSSPC and μPCD).

## 2. Sample preparation

Phosphorous-doped n-type amorphous silicon (*a*-Si:H) layers were deposited by PECVD (base pressure $10^{-7}$ mbar) on high quality p-doped (resistivity 1–3 Ω cm) monocrystalline Si (*c*-Si) wafers with <111> surface orientation and bulk diffusion lengths of several 100 μm. For experimental details, see e.g. [3,4]. *a*-Si:H/*c*-Si solar cells produced using the same PECVD system have yielded maximum efficiencies of 19.8% [6]. The investigated set of samples consists of ($n^+$)*a*-Si:H/(p)*c*-Si (*a*-Si:H doping $10^3$ ppm $PH_3$ in the gas phase) with increasing *a*-Si:H layer thickness (0.4 – 120 nm).

## 3. Experimental methods

### 3.1. Surface photovoltage

Surface photovoltage (SPV) is an electrical characterization technique that is well-established for the determination of the density of surface states especially at the silicon/silicon oxide interface [7]. The principle is described elsewhere [4,8] and will be briefly outlined here: The sample under test is sandwiched in a structure consisting of a transparent conductive front contact (TCO — typically zinc oxide), an

* Corresponding author. Tel.: +49 30 8062 1351.
*E-mail address:* korte@helmholtz-berlin.de (L. Korte).

0040-6090/$ – see front matter © 2009 Elsevier B.V. All rights reserved.
doi:10.1016/j.tsf.2009.02.090

**Table 1**
Parameters used in the numerical simulations with Silvaco ATLAS and AFORS-HET.

| | |
|---|---|
| *Silicon* | |
| Volume lifetime | 1 ms |
| Wafer thickness | 300 µm |
| Doping | p-type, $1\times10^{15}$/cm$^2$ |
| *Rear surface* | |
| ATLAS: constant surface recombination velocity | 1000 cm/s |
| AFORS-HET: insulator, $E_g=5$ eV | |
| *Defect on front side* | |
| Type | Donor |
| Density | $3\times10^{10}$/cm$^2$ |
| Hole capture cross section $\sigma_p$ | $1\times10^{-16}$ cm$^2$ |
| Electron capture cross section $\sigma_n$ | $1\times10^{-14}$ cm$^2$ |
| Energetic position | $E_V+0.45$ eV |
| *SPV — laser parameters* | |
| Wavelength | 910 nm |
| Pulse length | ATLAS: 150 ns<br>AFORS: 5–150 ns |
| Intensity | $\leq10^{22}$ Phot/(s cm$^2$) |

insulating slab of mica, the sample and a back contact. Thus, a metal–insulator–semiconductor structure (MIS) is created. Upon intense illumination of the sample by a short laser pulse ($\lambda=910$ nm, pulse duration 150 ns, maximum intensity $10^{19}$ photons/(cm$^2$ s)) through the TCO, excess charge carriers are generated in the sample, leading to a flattening of the bands and a split-up of the quasi-Fermi levels of electrons and holes. The redistributed charge in the sample changes the surface potential, which is measured capacitively via the insulator as a photovoltage pulse $V_{SPV}$. Ideally, the system has reached steady state when the laser pulse is switched off. The maximum value of the SPV signal right after the laser pulse, $V_{SPV}(t=0)$, is given by the difference of the surface potentials in the dark and under illumination. If the illumination intensity was high enough to reach flat-band conditions in the sample, $V_{SPV}(t=0)$ (corrected by the Dember voltage, see below) gives directly the surface band bending in the dark, $q\varphi_{s0}$. This is the case under high injection conditions, when charge carrier densities $n_{illum}$, $p_{illum} \gg n_{dark}$, $p_{dark}$. After the light pulse has ended, the decay of the light-induced excess carriers due to recombination in the bulk and at the interfaces leads to a relaxation of the surface band bending into its dark equilibrium state. Thus, the time-dependent measurement of the surface photovoltage transient $V_{SPV}(t)$ yields information on the recombination processes and associated rate constants in the bulk and at the surfaces and interfaces of the sample.

For the *a*-Si:H/*c*-Si samples investigated here, the chosen excitation wavelength of 910 nm corresponds to sub-bandgap light for the *a*-Si:H film ($E_{phot}=1.36$ eV$<E_{g,a\text{-Si:H}}\approx1.7$ eV). Thus, electron-hole pairs are generated in the *c*-Si substrate, and recharging of *a*-Si:H/*c*-Si interface or *a*-Si:H defect states should mainly occur through injection of electrons and holes from the *c*-Si into the thin *a*-Si:H film.

### 3.2. Numerical simulation

The numerical simulations have been carried out using the computer program AFORS-HET [9] which allows to simulate the output of measurement techniques for an arbitrary sequence of semiconducting layers and interfaces with an arbitrary number of defects. Since version 2.1, AFORS-HET is also capable of simulating transient effects, which is the basis for the present investigation. For some cases, a comparison with transient simulations using the commercial ATLAS device simulator from Silvaco® International was carried out to check the reliability of AFORS-HET's transient mode against a reference. However, it was found that the transient calculations using ATLAS did only converge to stable solutions for very small band bending at the *c*-Si surface.

The structure used in all simulations consisted of a 300 µm thick p-doped *c*-Si wafer with either a constant rear side recombination velocity of 1000 cm/s (a typical value for an oxide-covered *c*-Si surface) for the calculations using ATLAS, or with a 1 nm thin wide-gap semiconductor as insulating, $SiO_2$-like layer on the back ($E_g=5$ eV, i.e. below $E_{g,SiO2}$, for increased numerical stability) for the AFORS-HET simulations. Regarding the simulation results, both types of back surfaces lead to very similar results. This is to be expected, as the front surface recombination velocity for the simulated structure, calculated using the Shockley–Read–Hall formalism, is between ~$3\times10^4$ and ~350 cm/s at $\Delta n_s<10^{12}$ and $>10^{17}$ cm$^{-3}$, respectively, for the defect parameters chosen here. Thus, either the front surface recombination dominates (at low injection levels) or both interfaces contribute about equally (at high injection level, for the case of constant S = 1000 cm/s).

Based on the results of SPV measurements on the *a*-Si:H thickness series (see below), the gap defect states (*c*-Si dangling bonds and *a*-Si:H gap states) on the front of the wafer were lumped into a single donor-like defect in the band gap at $E_V+0.45$ eV, i.e. slightly below *c*-Si midgap. The recombination via this defect is described by the general time-dependent Shockley–Read–Hall formalism (e.g. [10] and references therein). In addition, a fixed charge on the sample surface is used to control the surface band bending. The presence of fixed charges on the *a*-Si:H surface also had to be assumed by Olibet et al. [11] to simulate correctly the dependence of effective lifetime vs. excess carrier density in QSSPC. The simulation parameters are summarized in Table 1.

## 4. Results and discussion

### 4.1. SPV on ($n^+$)*a*-Si:H/(p)*c*-Si structures with varying *a*-Si:H thickness

Fig. 1 shows the TR-SPV measurements for the series of ($n^+$)*a*-Si:H/(p)*c*-Si samples with varying *a*-Si:H thickness, together with the data obtained from an unprocessed wafer covered with native oxide. The light pulse ends at $t=0$ and is not resolved on the µs time scale.

For the *a*-Si:H/*c*-Si samples, all transients show a fast initial decay at $t<10$ µs. For the sample covered with 0.4 nm *a*-Si:H – a nominal layer thickness, the *a*-Si:H forms no closed film but islands on the *c*-Si at such low coverages [12] – the transient voltage then decreases quickly up to $t\approx40$ µs and subsequently tails off with a relatively small slope, as compared to the other samples. The sample covered with 4.3 nm *a*-Si:H already shows a plateau region for times $t<60$ µs after the light pulse, followed by a steep decrease to $V_{SPV}<10$ mV at $t>100$ µs. For all other samples with *a*-Si:H layer thicknesses of 6–

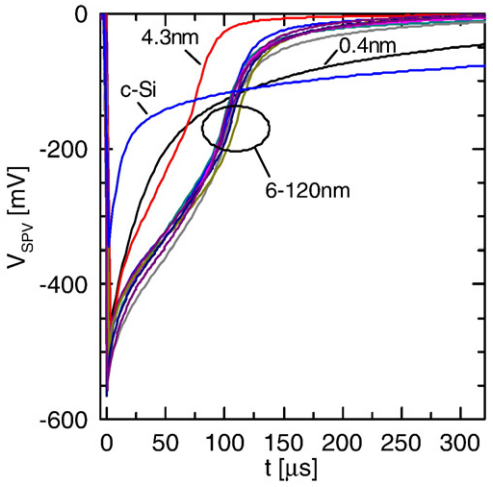


**Fig. 1.** Surface photovoltage transients measured on ($n^+$)*a*-Si:H/(p)*c*-Si structures for *a*-Si:H film thicknesses from 0.4 to 150 nm. A transient measured on the *c*-Si substrate covered by its native oxide is also included.

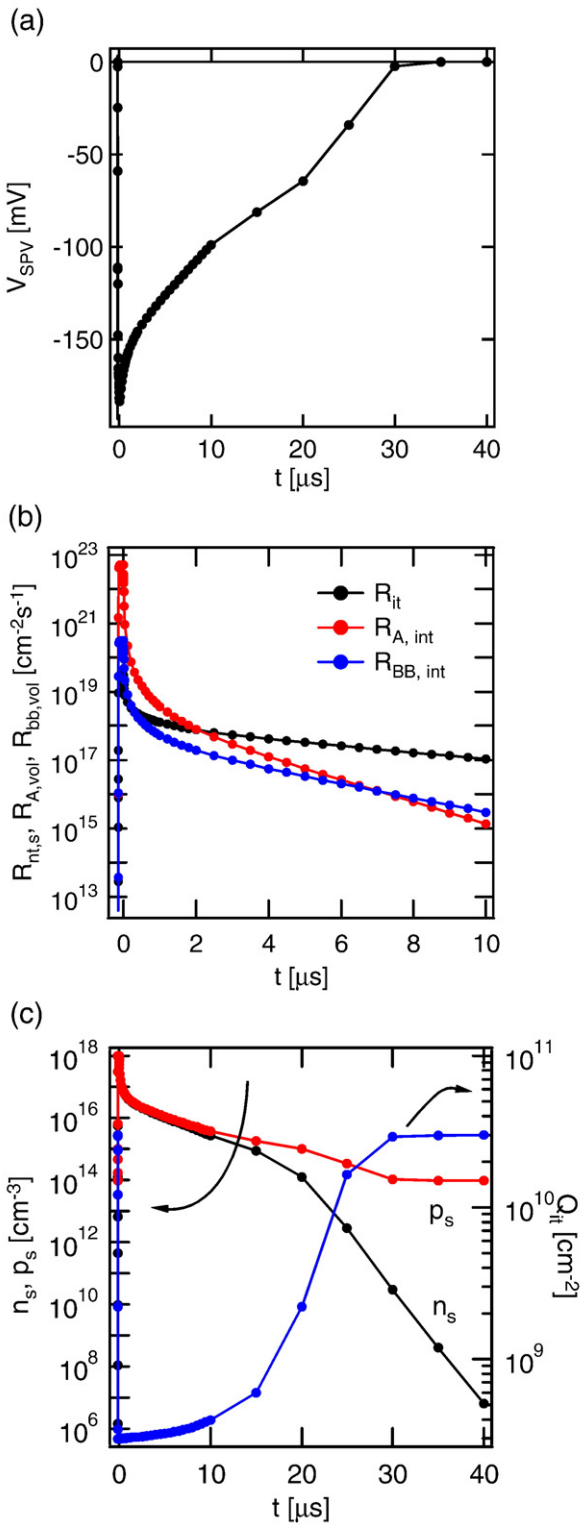


**Fig. 2.** a) Simulated surface photovoltage transient for a single donor-like defect level ($E_{it} = E_V + 0.45$ eV, $D_{it} = 3\times10^{10}$ cm$^{-2}$) on (p)*c*-Si. b) SRH recombination rate $R_{it}$ via the surface defect, Auger and band-to-band recombination rates $R_{A,int}$ and $R_{BB,int}$ integrated over the *c*-Si volume. c) Charge density $n_s$ and $p_s$ of electrons and holes at the surface, and density of trapped charge $Q_{it}$ in the surface state. Simulated excitation pulse: $\lambda = 910$ nm, $t_{Pulse} = 150$ ns, $\Phi_{Phot} = 10^{22}$ photons/(cm$^2$s).

120 nm, the general behaviour is similar, but the decrease in the plateau region, which now extends to $t \sim 100$ µs, is much slower.

These experimental results suggest that at least in moderately doped ($n^+$)*a*-Si:H layers, for *a*-Si:H layer thicknesses exceeding ~5 nm, *a*-Si:H/*c*-Si interface recombination is governed by the properties of both the interface itself and the first nm of *a*-Si:H adjacent to the interface. We have reported similar results already previously [4], and introduced the notion of an "effective interface" for the ensemble of the *a*-Si:H/*c*-Si interface and the adjacent *a*-Si:H within distances of the order of the tunnel length.

Based on the experimental finding reported in Fig. 1, we attempt to model the *a*-Si:H/*c*-Si samples by the simple structure proposed in the previous section, neglecting the properties of the *a*-Si:H completely and lumping all interface and *a*-Si:H properties into a single donor-type defect level with varying density $D_{it}$ [cm$^{-2}$]; additionally, the surface band bending in the system can be controlled by fixed charges $Q_{if}$ (i.e. non-rechargeable states that do not participate in the recombination process). $Q_{it}$ can be used to simulate the change in band bending due to varying doping in the *a*-Si:H. Obviously, this is a very crude model: In reality, both the *a*-Si:H/*c*-Si interface as well as the ultra-thin *a*-Si:H films exhibit continuous distributions of defect states, both donor- and acceptor-type, in the band gap [3,13]. In addition, it is generally accepted that *a*-Si:H dangling bonds are amphoteric defects, i.e. the same defect can be neutral, positively and negatively charged, with a shifted energetic position for the case of negative charge. This makes an extension of the standard Shockley–Read–Hall recombination model necessary, which was recently adapted also to the *a*-Si:H/*c*-Si interface [11]. Still, our model is sufficient to reproduce the general features of SPV transients (Fig. 1), as will be shown below. Because of the high degree of simplification, no attempt to extract quantitative values for defect densities, capture cross sections etc. from comparison between experimental (*a*-Si:H/*c*-Si) and simulated (single defect/*c*-Si) SPV transients will be made, though.

### 4.2 Features of the numerical model

We now explore the properties of our model, assuming a single donor-type defect state placed at $E_V + 0.45$ eV, with a density of $D_{it} = 3\cdot10^{10}$ cm$^{-2}$. Note that this is the correct type of defect for this energetic position, as in contrast to volume defects, surface states are donor-like at $E_{it} < E_g/2$ (and acceptor-like at $E_{it} > E_g/2$). $D_{it}$ and the energetic position are chosen somewhat arbitrarily, the main reason for this choice being issues with the numerical stability of the transient calculations using the ATLAS software.

With these parameters, the structure has a moderate surface band bending of 211 meV. Fig. 2a) shows its reaction to a rectangular illumination pulse at $\lambda = 910$ nm, $t_{Pulse} = 150$ ns, with a maximum intensity of $10^{22}$ photons/(cm$^2$ s). Clearly, the distinct features of the SPV transients measured on *a*-Si:H/*c*-Si structures (Fig. 1) are reproduced. From the model calculations, a deeper insight into the dominant recombination mechanisms can be obtained: The contribution of recombination at the surface defects as compared to the Auger and band-to-band recombination is displayed in Fig. 2b. This graph clearly shows, that recombination via surface defects is dominant for $t > 2$ µs. For $t < 2$ µs, the decay of excess charge density is governed by Auger recombination in the *c*-Si bulk. This correlates well with the transition of the SPV voltage (Fig. 2a) from steep decrease into a plateau. Finally, in Fig. 2c, the charge state of the surface defects is depicted over time. Here, the reason for the kink in the $V_{SPV}(t)$ transient at $t \sim 20$ µs after the end of the light pulse becomes clear: Under dark equilibrium conditions, the surface states are ionized, i.e. positively charged, because the surface Fermi level lies below the energetic position of the defects. Upon illumination, the quasi Fermi level of the electrons sweeps over the defect energy level, the donor-type states are occupied by electron and thus neutralized: The charge in surface states drops by two orders of magnitude under the chosen illumination conditions. When, at $t \sim 20$ µs after the pulse, recombination has proceeded up to the point where the system leaves the high injection region (i.e. when $n_s$ and

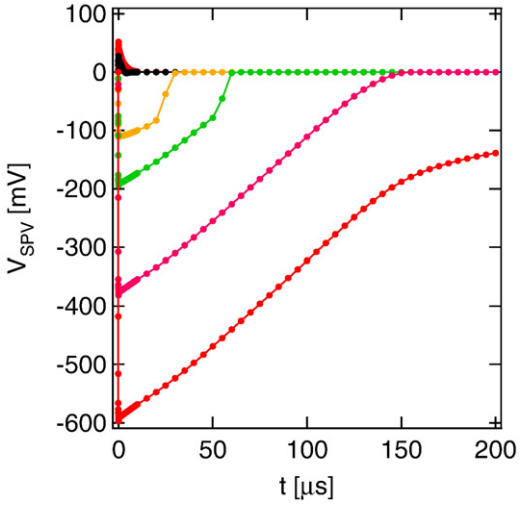


**Fig. 3.** Simulation: Change of surface photovoltage transients for different band bending at the *c*-Si surface. The band bending was varied by changing the additional fixed interface charge $Q_{if}$ between $-1.5\times10^{11}$ cm$^{-2}$ and $+1\times10^{11}$ cm$^{-2}$. Defect parameters ($D_{it}=3\times10^{10}$ cm$^{-2}$, $E_{it}=E_V+0.45$ eV) and excitation conditions were kept identical.

$p_s$ start to diverge) and the quasi Fermi level positions change rapidly again, the defect states are ionized again. The change in defect charge state leads to an accelerated change in surface band bending, and thus a fast decrease of $V_{SPV}$. Generally, to reproduce the kink in the transient, we find that it is necessary to assume surface defects that are recharged during the transient — the simple assumption of a surface recombination velocity independent of excess carrier density leads to a featureless decay transient. The simulated transient in Fig. 3 illustrates this again. Here, the dark equilibrium surface band bending $q\varphi_{s0}$ was varied between +100 and −600 meV, by introducing additional fixed surface charges $Q_{if}$. Note that the same effect can be achieved by applying an external bias voltage to the sample under test, a method used in voltage dependent SPV measurements (VD-SPV), or by (accidentally) introducing an electrostatic charge on the insulating mica foil. For surface band bending significantly (i.e. some $k_bT$) above 450 meV (lower two curves), the donor-like defect at $E_V+450$ meV is occupied by electrons and thus neutral at all times, both during illumination and while $V_{SPV}$ decays. Under these circumstances, an almost linear SPV decay is observed in the simulation. It is also worth noting that at least for the higher band bending values, the slope of the $V_{SPV}$ decay in the 'plateau' region (before significant defect recharging occurs) is virtually unchanged for different band bendings.

### 4.3 Change of SPV transient with varying photon flux

In Fig. 4, we show experimental surface photovoltage transients measured on a 10 nm (n$^+$)*a*-Si:H/(p)*c*-Si sample, where the photon flux $\Phi_{Ph}$ incident on the sample was varied between $10^{15}$ and $10^{19}$ cm$^{-2}$ s$^{-1}$. Three features are most notable in these transients: a) The initial fast decay, shown above to be related to Auger recombination processes, sets in only at photon fluxes above $10^{17}$ photons/(cm$^2$s), b) the initial SPV voltage, at $t=0$, almost saturates at high excitation intensities, and c) the plateau, i.e. the region of the transient between the Auger dominated steep decrease and the 'kink' at ~40–70 µs, appears only at $\Phi_{Ph}>10^{17}$ cm$^{-2}$ s$^{-1}$, widens and becomes less steep with increasing photon flux. The proposed numerical model can reproduce this behaviour: In Fig. 5, simulated transients are shown with photon flux varying from $10^{10}$ to $10^{23}$ cm$^{-2}$ s$^{-1}$. At $\Phi_{Ph}=10^{19}$ cm$^{-2}$ s$^{-1}$, the plateau starts to develop, and for $\Phi_{Ph}\geq10^{20}$ cm$^{-2}$ s$^{-1}$, there is an appreciable contribution from Auger recombination, leading to the initial fast decrease. Generally, the photon fluxes needed for producing similar features (Auger peak, plateau) in the simulation are ~1–2 orders of magnitude higher than in the experiment. This may most likely be due to the simplicity of the proposed defect model and will be investigated further. The inset of Fig. 5 shows the dependence of $V_{SPV}(t=0)$ on $\Phi_{Ph}$. The graph shows that indeed, the simulated maximum photovoltage is, for high photon fluxes, close to the initial surface band bending in the dark: The maximum photovoltage reached in the simulations is $V_{SPV}(t=0;\ \Phi_0=10^{22}$ photons/(cm$^2$s)$)=-184$ mV; while the band bending in the dark is −211 mV. This discrepancy is reduced when the transients are corrected for the contribution coming from the so-called Dember voltage that arises from the mobility difference of electrons and holes [14]. This quantity can easily be calculated if the excess charge carrier density is known. The inset of Fig. 5 shows the uncorrected (open circles) and Dember-corrected (filled circles) $V_{SPV}(t=0)$ in dependence of the illumination density. For $\Phi_0=10^{22}$ photons/(cm$^2$s)), the Dember-corrected photovoltage is $V_{SPV}(t=0)=-199$ mV. Thus, one can conclude for the experiment, that the measured surface photovoltage $V_{SPV}(t=0)$ indeed yields a value close to the *c*-Si dark band bending (error <10% in the present simulation), provided that the excitation conditions are sufficient to reach the high excitation regime, where $n_{ill}$, $p_{ill}\gg n_{dark}$, $p_{dark}$. The appearance of the Auger peak at short times after the illumination pulse can be considered a qualitative indicator that the high injection region is indeed reached.

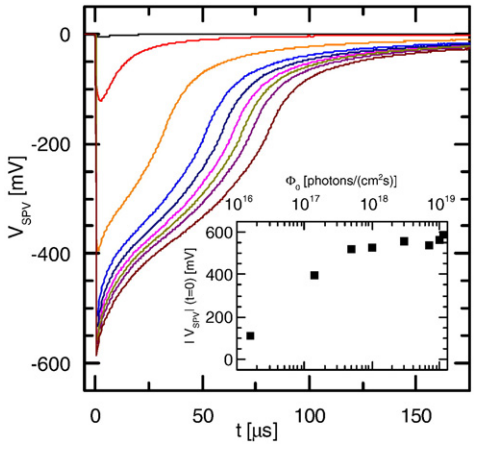


**Fig. 4.** Experimental SPV transients ($t_{Pulse}=150$ ns, $\lambda=910$ nm) for varying illumination photon flux, $\Phi_{Ph}=10^{15}$–$10^{19}$ photons/(cm$^2$s), obtained from a (n)*a*-Si:H/(p)*c*-Si structure. Inset: $V_{SPV}(t=0)$ (i.e. immediately after the end of the light pulse) vs. photon flux $\Phi_0$.

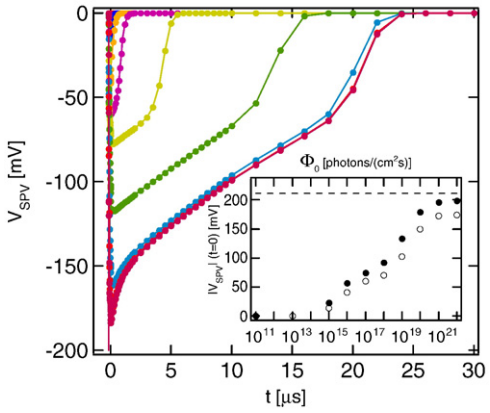


**Fig. 5.** Time dependence of simulated SPV transients for *c*-Si with a donor-type surface defect at a density of $3\times10^{10}$ cm$^{-2}$ and varying incident photon flux, from $\Phi_{Ph}=10^{11}$ to $10^{22}$ cm$^{-2}$ s$^{-1}$. Inset: $V_{SPV}(t=0)$ (i.e. immediately after the end of the light pulse) vs. photon flux $\Phi_0$, uncorrected (open circles) and Dember-corrected (filled circles). The dashed line marks the surface band bending $q\varphi_{s0}$ in the dark.

## 5. Conclusions

Motivated by the experimental finding that in *a*-Si:H/*c*-Si heterojunctions, only the first ~10 nm of *a*-Si:H close to the heterointerface contribute to the interface recombination properties as probed by time-resolved surface photovoltage (TR-SPV), we use a very simple surface defect model to describe successfully all the principal features of TR-SPV measurements. The simulation shows that at under high excitation conditions, Auger recombination governs the initial SPV decay after the light pulse is switched off. Experimentally, two distinct types of further decay characteristics are found: One with a quasi-linear decay down to photovoltages of a few percent of the initial SPV voltage $V_{SPV}(t=0)$, the other one with a kink in the $V_{SPV}(t)$ curve and a subsequent fast decay. The simulation results show unambiguously, that the kink occurs only for those cases where interface defect states have changed their charge state significantly during illumination, the kink occurring when they return to their dark equilibrium state. This happens at the transition of the surface from high- to low injection conditions. In addition, the numerical simulation of the transient should allow, in principle, to calculate the minority excess charge carrier density $\Delta n(t;\ x=0)$ at the *c*-Si surface or the *a*-Si:H/*c*-Si interface over time, which will make possible the extraction of recombination properties (energetic position, recombination velocities) of the interface states. The system of band gap defect states at the *a*-Si:H/*c*-Si interface, consisting of the heterointerface itself and the *a*-Si:H adjacent to the interface up to a distance of the order of the tunnel length, with continuous distributions of defect states both at the interface and in the *a*-Si:H, is far more complex than our model, though. Therefore, we refrain in this work from a quantitative comparison of experiment and model, and from extracting interface defect properties from the simulations.

It should be noted that, as compared to techniques such as quasi-steady state photoconductance (QSSPC), for SPV, it is (a) not necessary to use symmetric sample structures, and (b) the technique is also able to investigate heterojunctions (or surface states) of very thin substrates (where for QSSPC, not enough substrate material is present to inductively detect excess charge carriers), provided that excitation at sufficiently short wavelengths is available and leads to a measurable band bending. This makes SPV a method that is especially interesting for the investigation of thin film (solar cell) materials. Concerning the proposed numerical model, a refinement including more realistic defect distributions, an actual *a*-Si:H layer on the *c*-Si, and mechanisms such as tunnelling of charge carriers through the interface, is under investigation.

## Acknowledgements

We thank K. Jacob and S. Scheu for *c*-Si wafer pre-cleaning, E. Conrad for *a*-Si:H depositions and D. Patzek for additional SPV measurements. This work has been partially funded by the European Commission through the FP7 project “Heterojunction Solar Cells based on a-Si c-Si” (HETSI), grant agreement no. 211821.

## References

[1] A. Froitzheim, K. Brendel, L. Elstner, W. Fuhs, K. Kliefoth, M. Schmidt, J. Non-Cryst. Solids 299–302 (2002) 663.
[2] H. Angermann, L. Korte, J. Rappich, D. Schaffarzik, E. Conrad, I. Sieber, M. Schmidt, Proc. 22nd European Photovoltaic Solar Energy Conference, 2007, p. 2089.
[3] L. Korte, M. Schmidt, J. Non-Cryst. Solids 354 (2008) 2138.
[4] A. Laades, K. Kliefoth, L. Korte, K. Brendel, R. Stangl, M. Schmidt, W. Fuhs, 19th European Photovoltaic Solar Energy Conf., 2004, p. 1170.
[5] D. Schaffarzik, R. Stangl, A. Laades, C. Schubert, M. Schmidt, Proc 22nd European Photovoltaic Solar Energy Conf., 2007, p. 1224.
[6] E. Conrad, L. Korte, K.v. Maydell, H. Angermann, C. Schubert, R. Stangl, M. Schmidt, Proc. 21st European Photovoltaic Solar Energy Conf., 2006, p. 784.
[7] Y.W. Lam, J. Phys. D: Appl. Phys. 4 (1971) 1370.
[8] W. Füssel, M. Schmidt, H. Angermann, G. Mende, H. Flietner, Nucl. Instrum. Methods Phys. Res. A 377 (1996) 177.
[9] R. Stangl, M. Kriegel, D. Schaffarzik, M. Schmidt, Technical Digest 15th Int. Photovoltaic Science and Engineering Conf. (PVSEC-15), Shanghai, 2005, p. 985.
[10] J.W. Orton, P. Blood, The Electrical Characterization of Semiconductors: Measurement of Minority Carrier Properties, Academic Press, London, 1990, p. 15ff.
[11] S. Olibet, E. Vallat-Sauvain, C. Ballif, Phys. Rev. B 76 (2007) 035326.
[12] I. An, H. Nguyen, N. Nguyen, R. Collins, Phys. Rev. Lett. 65 (1990) 2274.
[13] H. Angermann, W. Henrion, M. Rebien, J.T. Zettler, A. Röseler, Surf. Sci. 388 (1997) 15.
[14] K. Heilig, Solid State Electron. 21 (1978) 975.